Field-Embedded Particles Driven by Active Flips

Ruben Zakine, Jean-Baptiste Fournier, and Frédéric van Wijland
Laboratoire Matière et Systèmes Complexes (MSC), Université Paris Diderot, USPC, UMR 7057 CNRS, F-75205 Paris, France

(Received 22 January 2018; revised manuscript received 6 April 2018; published 10 July 2018)

Systems of independent active particles embedded into a fluctuating environment are relevant to many areas of soft-matter science. We use a minimal model of noninteracting spin-carrying Brownian particles in a Gaussian field and show that activity-driven spin dynamics leads to patterned order. We find that the competition between mediated interactions and active noise alone can yield such diverse behaviors as phase transitions and microphase separation, from lamellar up to hexagonal ordering of clusters of opposite magnetization. These rest on complex multibody interactions. We find regimes of stationary patterns, but also dynamical regimes of relentless birth and growth of lumps of magnetization opposite of the surrounding one. Our approach combines Monte Carlo simulations with analytical methods based on dynamical density functional approaches.

DOI: 10.1103/PhysRevLett.121.028001

Active matter encompasses a broad class of physical systems, ranging from animal flocks [1–4], artificial self-propelled particles [5,6], and bacteria [7] to molecular motors [8], and pumping [9,10] or multistate particles such as proteins [11]. While the former share the ability to extract energy from their environment and to convert it into directed motion, the latter can change conformation and exert active forces upon their surrounding medium (actin filaments, cell membrane). Particles that deform a correlated elastic medium experience field-mediated interactions with a fluctuation-induced component [12,13], as illustrated in Fig. 1. Mediated interactions occur, for instance, between interfaces, colloids, or proteins in soft-matter media such as critical binary mixtures [14,15], liquid crystals [16,17], capillary interfaces [18,19], and biomembranes [20–24], including in nonequilibrium settings [25].

An early approach to the question of why and how active particles, e.g., proteins in cell membranes, self-organize appeared in [11,26,27]. In a parallel series of works on reactive two-state particle systems, spinodal decomposition coupled to active flips between the states has been shown to lead to a wealth of complex patterns. These have been described in [28–33]. A common feature to these approaches, necessary for the active flips to produce nontrivial patterns, is the requirement to start from directly interacting objects, either by assuming two-body interactions or in a coarse-grained form by describing these in terms of an *ad hoc* Cahn-Hilliard field.

In this Letter, we show that the emergence of activity-driven patterns can arise from purely field-mediated interactions, in the absence of any direct interactions between the particles. The nature of the coupling between the particles and the field is essential, as the existence of nonequilibrium phase transitions completely rests on the physics governing the coupling. Furthermore, out of equilibrium, the coupling of particles to a field cannot be interpreted as effective direct interactions between particles. We concentrate on systems whose only nonequilibrium character resides in the active switching of the particles between two states coupling differently to the medium's field. Such systems can be found both in biophysics and in soft matter: adenosine triphosphate (ATP)-binding cassette transporters, for instance, are ATP-controlled transmembrane proteins that actively locally remodel the membrane shape [34,35]. Other examples include *p*H-driven KcsA potassium channel proteins

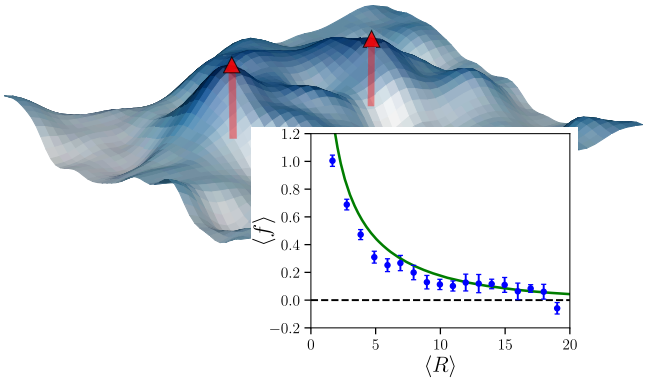

FIG. 1. Two particles (up spins) coupled to a fluctuating field (surface plot), favoring some value ϕ_0 of the field. (Inset) Equilibrium average force as a function of the average particle separation, for the Hamiltonian described in the text. One particle is held fixed and the other one is tethered to a strong harmonic trap. (Symbols) Results of the numeric simulation (with incertitude). (Solid line) Analytical force deriving from $U(R)$ in the text. (Parameters) $r = 0.01$, $\phi_0 = 8$, $B = 1$, and $\mu = 0.05$.

that are believed to couple to the membrane thickness [36], laser-induced virtual colloids in nematic liquid crystals [37], or optically switchable bistable colloids in chiral liquid crystals [38]. We do not rely on a simplified field–particle-density coupling. We treat the field-particle interactions at the microscopic level (background illustration in Fig. 1), in order to capture multibody contributions and Casimir-like effects.

In order to investigate such phenomena, we have striven to build up a model relying on the minimal necessary ingredients: two populations of independent diffusing Ising particles, actively switching between their two states and interacting (quadratically) with a background Gaussian field, make up our model system. We refer to these particles as active switching field interacting particles (ASFIPs). The complexity of this system rests on the active nature of the particles, but also on the dynamics of the field-mediated interactions. We treat the dynamics of each particle and that of the field by equilibrium Langevin equations. The questions we ask are the following: (i) Are induced interactions coupled to activity sufficient to generate emerging cooperative phenomena? (ii) What is the role of activity (in as much as it drives us away from equilibrium) in generating complex patterns? (iii) What is the role of multibody interactions and of Casimir-like forces in the states of matter that we observe?

We consider N noninteracting particles at positions $\boldsymbol{r}_k(t)$, $1 \leq k \leq N$, embedded in a medium whose elasticity is described by a scalar Gaussian field $\phi(\boldsymbol{x}, t)$. Our field ϕ might refer to a biomembrane thickness [21,23] or internal lipid composition [39]. It may also refer to the shape of a biomembrane [20,22] or to that of an interface under gravity [18,19]. While all these systems are well described by Gaussian fluctuating fields, the specifics of the Hamiltonian is model dependent. We choose the simplest model, with energy

$$H_0 = \int d^2x \left[\frac{r}{2}\phi^2 + \frac{c}{2}(\boldsymbol{\nabla}\phi)^2\right]. \tag{1}$$

To model particles that can be in two states, we attach a spin variable $S_k = \pm 1$ to each particle. The underlying picture we have in mind is that of protein inclusions changing conformation through external chemical activity [40]. The particle-field coupling is a key ingredient; we take

$$H_{\text{int}} = \sum_{k=1}^{N} \frac{B}{2}[\phi(\boldsymbol{r}_k) - S_k\phi_0]^2. \tag{2}$$

The effect of this interaction is to adjust locally the field to a spin-dependent amplitude $\pm\phi_0$, with a strength governed by the stiffness coefficient B. We draw the reader's attention to the quadratic nature of H_{int}. Linear couplings in the field are quite unrealistic as they miss multibody and fluctuation-induced interactions due to linear superposition of the deformation field. By contrast, a quadratic coupling constrains the field at the particle location, which prevents linear superposition and generates multibody interactions and Casimir-like forces. We do not wish to discard such ingredients that exist in real systems. The total energy becomes $H = H_0 + H_{\text{int}}$. We purposely omit excluded volume or any other kind of direct interaction, which allows us to witness field-induced phenomena only. Note that, depending on the physical context, a coupling involving higher derivatives of the field could be considered (e.g., for curvature-inducing proteins).

We endow ϕ with a purely relaxational dynamics satisfying detailed balance

$$\partial_t\phi(\boldsymbol{x}, t) = -\Gamma\frac{\delta H}{\delta\phi(\boldsymbol{x}, t)} + \sqrt{2\Gamma T}\xi(\boldsymbol{x}, t), \tag{3}$$

where T is the temperature in energy units, Γ is the field mobility, and $\xi(\boldsymbol{x}, t)$ is a Gaussian white noise. Particles diffuse according to equilibrium overdamped Langevin equations

$$\frac{d\boldsymbol{r}_k}{dt} = -\mu\frac{\partial H}{\partial \boldsymbol{r}_k} + \sqrt{2\mu T}\boldsymbol{\eta}_k(t), \tag{4}$$

where μ is a mobility coefficient (assumed to be spin and field independent), and the $\boldsymbol{\eta}_k(t)$'s are independent Gaussian white noises. We use the simplifying assumption that $\boldsymbol{\eta}_k$ and ξ are independent (as is generic in soft matter, see, e.g., Ref. [10] for proteins in biomembranes).

Finally, the out-of-equilibrium dynamics arises from the internal degree of freedom of the particles. Each particle flips through the action of an external energy source (e.g., photons, chemical reactions), with fixed rates

$$S_k = -1 \underset{\gamma}{\overset{\alpha}{\rightleftharpoons}} S_k = +1 \quad \text{(ASFIP)}. \tag{5}$$

This is the one process breaking detailed balance for ASFIPs due to the coupling with the field and particle dynamics.

Since we want to understand how our system behaves exactly, taking into account detailed out-of-equilibrium mediated interactions and multibody and fluctuation-induced effects without relying on approximate analytical methods, we first perform Monte Carlo simulations. We discretize our equations on a lattice with spacing a, with the normalization $a = T = \Gamma = c = 1$ (see Supplemental Material, Sec. I [41]). The remaining parameters are r, fixing the field's correlation length $r^{-1/2}$, B the stiffness of the spin-field coupling, ϕ_0 the targeted field, and the dynamical parameters μ, α, and γ, all scaled by the field's mobility.

We implement discrete-time Monte Carlo simulations on a two-dimensional (2D) square lattice of size $L \times L$ with periodic boundary conditions, as detailed in the

Supplemental Material (Sec. II) [41]. The field is defined on the lattice sites and the particles move from site to adjacent site. Between times t and $t+\Delta t$, particles can hop, or flip spin, or stay on the same site. To take into account the relative dynamics of the particles and the field, we implement a tower sampling algorithm [42] instead of a Metropolis one.

In order to characterize the field-mediated interaction in equilibrium, we first study the force exchanged by two particles a distance R apart in the manner described in Fig. 1 (or Sec. III in Supplemental Material for a precise description [41]). The effective potential $U(R)$ between these two particles can be derived (see Supplemental Material) from a field-theoretic calculation. As shown in Fig. 1, the force is well fitted by $U'(R)$, which confirms the validity of our Monte Carlo simulation. The force is attractive for equal spins and decays typically over the field correlation length. We found that for $R \geq 1$ and $\phi_0 \gtrsim 3$ the fluctuation-induced component of the force is negligible with respect to the elastic component, but this does not mean that it must be so out of equilibrium. Actually, the standard deviation of the force, which has a component coming from the Langevin force on the particle and another coming from the fluctuations of the field, is much larger than its average. Note that, whereas in equilibrium the field samples thermally all of its configurations (even when the particles move), in the out-of-equilibrium case, the dynamics of the field could yield memory effects with important consequences.

Before we embark into a full description of the out-of-equilibrium ASFIPs, we wish to introduce their equilibrium counterpart, for future comparison purposes. In equilibrium, switching field interacting particles (SFIPs) have transition rates $\propto \exp(\pm w_k)$ with $w_k = B\phi_0\phi(\boldsymbol{r}_k)$ half the energy variation in a spin flip. Such particles experience equilibrium field-mediated interactions and flips, while they diffuse on the lattice. Let N be the total number of particles and $\rho_0 = N/L^2$. At fixed r and ϕ_0, we increase the coupling strength B. We observe first a paramagnetic-ferromagnetic phase transition [Fig. 2(a)], then a phase separation into a dense ferromagnetic fluid coexisting with a paramagnetic gas [Fig. 2(b)]. These states obviously do not depend on the dynamical parameter μ. We characterize the magnetization of each homogeneous phase by the order parameter $\psi = \langle \rho^+ - \rho^- \rangle / \langle \rho \rangle$, where $\rho^\pm$ is the density of particles with ± 1 spins and $\rho = \rho^+ + \rho^-$, and we find that the paramagnetic-ferromagnetic phase transition is compatible with a continuous one [Fig. 2(a), inset].

Since SFIPs are in equilibrium, we can rely on thermodynamics to study their behavior. The mean-field energy density naturally deriving from H is

$$f_{\mathrm{MF}} = \frac{r}{2}\phi^2 + \frac{B}{2}\rho^+(\phi-\phi_0)^2 + \frac{B}{2}(\rho-\rho^+)(\phi+\phi_0)^2 + \rho^+ \ln \rho^+ + (\rho-\rho^+)\ln(\rho-\rho^+). \quad (6)$$

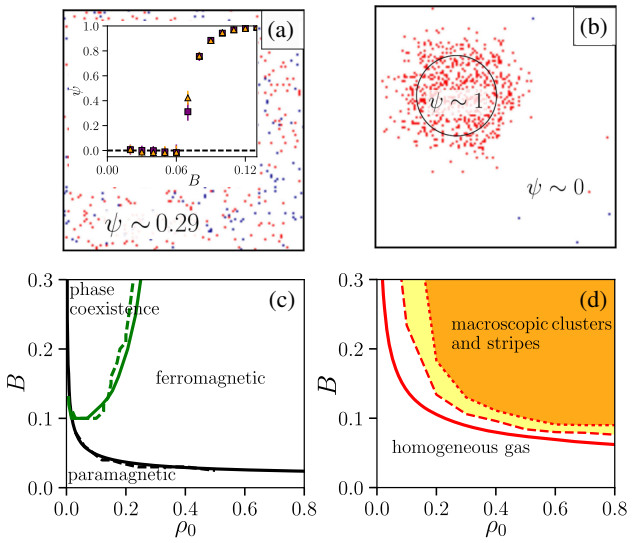

FIG. 2. (a) SFIPs in a box with periodic boundary conditions $L = 150$, $\rho_0 = 0.05$, $r = 0.01$, $\phi_0 = 8$, and $B = 0.07$, yielding a ferromagnetic state. Red (blue) dots indicate particles with up (down) spins. (Inset) Magnetization order parameter as a function of B. Light orange (dark purple) symbols correspond to B increasing (decreasing). (b) SFIPs for $B = 0.26$ (same other parameters) showing the coexistence of a ferromagnetic liquid and a paramagnetic gas. (c) Phase diagram of SFIPs in terms of total density and coupling strength for $r = 0.01$, $\phi_0 = 8$, and $\mu = 5$. (Solid lines) Mean-field predictions for the paramagnetic-ferromagnetic transition (black) and for the binodal curve of the phase separation (green or gray). The corresponding dashed lines are the results of the Monte Carlo simulations. (d) ASFIPs for the same parameters and $\alpha = \gamma = 0.1$. (Solid red line) Mean-field prediction for the transition to a patterned phase. [Yellow (light gray) zone] Beginning of segregation. [Orange (gray) zone] Ferromagnetic stripes and macroscopic clusters.

Since ρ is the only conserved quantity, we minimize f_{MF} with respect to ϕ and ρ^+, which yields an energy density $f'_{\mathrm{MF}}(\rho)$ and $\phi = B\phi_0(2\rho^+ - \rho)/(r + B\rho)$ with either $\rho^+ = \rho^- = \rho/2$ (paramagnetic phase) or $\rho^+ \neq \rho^-$ (ferromagnetic phase). At low values of B, the system is uniform and there is a continuous paramagnetic-ferromagnetic transition at $B_c^{(\mathrm{MF})} = (1 + \sqrt{1 + 4r\phi_0^2/\rho_0})/(2\phi_0^2)$. At higher values of B, we obtain, through the double tangent construction on $f'_{\mathrm{MF}}(\rho)$, a phase separation between a low density paramagnetic phase and a high density ferromagnetic phase. These mean-field predictions correspond to the continuous lines of Fig. 2(c), while the results of the Monte Carlo simulations are indicated by the dashed lines. We have checked that the agreement is all the better as we are working at large ϕ_0 or low T.

We now return to our original nonequilibrium ASFIPs. The phase diagram of ASFIPs undergoing symmetric flips ($\alpha = \gamma$) is shown in Fig. 2(d). The system is always paramagnetic on global average, due to the imposed flips, however, increasing B at fixed ρ_0 yields first a transition from a paramagnetic gas to ferromagnetic clusters of either

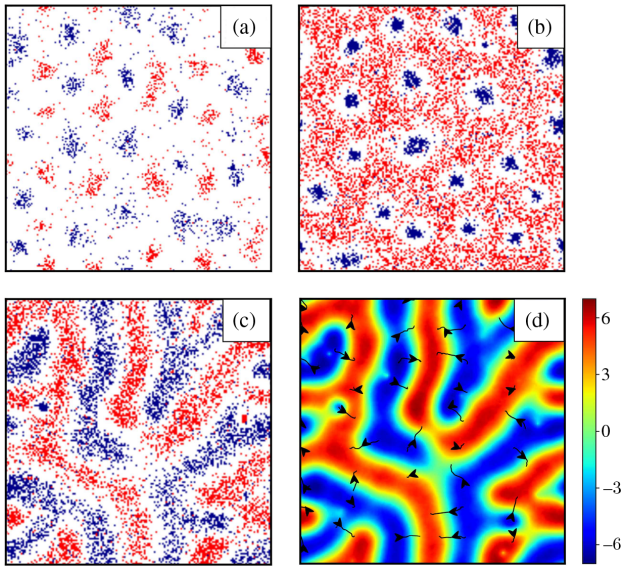

FIG. 3. Snapshots of the patterns created by ASFIPs. The parameters are $r = 0.01$, $\phi_0 = 8$. Red (blue) dots indicate particles with up (down) spins. (a) Square phase obtained for symmetric flips ($B = 0.26$, $\rho_0 = 0.1$, $\mu = 2.5$, $\gamma = \alpha = 0.005$, $L = 180$). (b) Hexagonal phase of clusters ($B = 0.15$, $\rho_0 = 0.4$, $\mu = 5.0$, $\alpha = 0.02$, $\gamma = \alpha/3$, $L = 160$). (c) Striped phase obtained for symmetric flips ($B = 0.15$, $\rho_0 = 0.4$, $\mu = 5.0$, $\gamma = \alpha = 0.02$, $L = 160$). (d) The corresponding ϕ field map of (c) and the time average of the fluxes of spin-up particles.

magnetizations, as illustrated in Fig. 3(a), then to a phase of dynamical ferromagnetic stripes. A typical snapshot of the macroscopic stripes is shown in Fig. 3(c). For asymmetric flips (e.g., $\alpha = 3\gamma$), we observe a dynamical hexagonal pattern of clusters [Fig. 3(b)]. These clusters are formed by the particles with the higher flip rate.

Mechanism.—Think of a system prepared with all spins up. Allow for activity to start flipping spins. Down spins will locally create a field depression that will diffuse around and harvest similar down spins. Lumps of down spins will grow by ripening and by coalescence. Their growth is limited by the symmetric process involving the birth of up spin inside. This scenario will result in a local dynamical pattern akin to microphase separation. Once in such a state, we have computed the average fluxes of the particles and the map of the ϕ field [Fig. 3(d)]. High (low) field regions have a majority of spin-up (spin-down) particles. Then, spin-up particles travel from regions of low spin-up density to regions of high spin-up density. However, these activity-driven fluxes never vanish, which is specific to being out of equilibrium. Therefore, whenever a particle flips, it is expelled by the field-mediated interactions towards the nearest region matching its updated spin. Within large enough regions of a given magnetization, we observe the systematic nucleation and growth of aforementioned lumps of opposite magnetization [e.g., small visible blue islands in Fig. 3(b) or red and blue ones in Fig. 3(c)], as illustrated by the videos in the Supplemental Material (Sec. V) [41].

What is the importance of fluctuation-induced interactions and multibody effects in the ASFIP system? If we turn off the field noise $\xi(\boldsymbol{x}, t)$ (while keeping the dynamics on the particles unchanged), we observe that particle segregation and pattern formation occur as soon as B exceeds the mean-field threshold [solid red line in Fig. 2(d)]. Thermal fluctuations tend to destroy patterns and fluctuation-induced forces are too weak to play any pattern-favoring role. In order to investigate multibody effects, we have also replaced the quadratic coupling of Eq. (2) with a linear coupling adjusted to yield, up to a very good approximation, the same two-body field-mediated interaction (see Supplemental Material [41]). This results in the condensation of the particles on a unique site for SFIPs and in the absence of activity-driven patterns for ASFIPs. Multibody interactions are thus essential. We have checked that adding a hard-core repulsion, in the quadratic coupling case, has almost no effect on the phase diagram, indicating that modest short-range interactions are irrelevant in our system.

Let us rationalize our findings on the phase diagram with a dynamical mean-field approach. Since ASFIPs diffuse by means of overdamped Langevin equations, we implement a Dean-Kawasaki [43,44] approach in the noiseless limit. The evolution equations then read $\partial_t \rho^{\pm} + \boldsymbol{\nabla} \cdot \boldsymbol{j}^{\pm} = 0$ with $\boldsymbol{j}^{\pm} = -\mu \rho^{\pm} \boldsymbol{\nabla}(\partial f_{\mathrm{MF}}/\partial \rho^{\pm})$. Taking spin exchange into account, we arrive at the evolution equations

$$\partial_t \rho^{\pm} = \mu \nabla^2 \rho^{\pm} + \mu B \boldsymbol{\nabla} \cdot [\rho^{\pm}(\phi \mp \phi_0) \boldsymbol{\nabla} \phi] \pm \alpha \rho^{-} \mp \gamma \rho^{+},$$
$$\partial_t \phi = \nabla^2 \phi - r\phi - B\rho^{+}(\phi - \phi_0) - B\rho^{-}(\phi + \phi_0). \qquad (7)$$

Linear stability analysis (LSA) shows that above a threshold in B the stationary and homogeneous solution $[\rho_s^{+} = \rho_0 \alpha/(\alpha + \gamma), \quad \rho_s^{-} = \rho_0 \gamma/(\alpha + \gamma), \quad \text{and} \quad \phi_s = B\phi_0(\rho_s^{+} - \rho_s^{-})/(r + B\rho_0)]$ is no longer stable, indicating the onset of a patterned phase. For symmetric flips, $\gamma = \alpha$, this threshold reads $B_a^{(\mathrm{MF})} = (1 + \sqrt{1 + 4r\phi_0^2/\rho_0 + 4\phi_0 s} + 2\phi_0 s)/(2\phi_0^2)$, where $s = \sqrt{2\alpha/(\mu\rho_0)}$. The agreement with the results of the Monte Carlo simulations is satisfying [Fig. 2(d)].

In dimensionful form, $B_a^{(\mathrm{MF})}$ turns out to be independent of the field mobility Γ. We have checked this property in the Monte Carlo simulations and found indeed that varying Γ over 5 orders of magnitude has no effect on the phase diagram. The timescales involved in the pattern formation, however, depend on Γ. In addition, LSA yields an interval of wave vectors over which the homogeneous solution becomes unstable. The pattern sizes we observe are consistent with the LSA predictions, including the fact that varying dynamical parameters Γ or μ and α, while keeping s constant, does not alter their size. We also found that increasing the particles' mobility μ (while keeping all other parameters fixed) enlarges the domain where patterns are stable in the phase diagram. Furthermore, LSA confirms that patterns are specific to out of equilibrium, since

sending $s \to 0$ yields opens up the instability interval down to zero wave vectors, ending up with a more conventional coarsening of the binary mixture in that regime.

We are now in a position to summarize the answers to our original questions. Starting from a microscopic model where *noninteracting* particles are coupled to a Gaussian field, we have proved that field-mediated interactions combined with activity can generate a wealth of new emerging cooperative phenomena. This is relevant for soft-matter systems in which interactions are mostly indirect and field mediated. In our system, it is the presence of activity that drives complex patterns of particle clusters by a continuous tossing in and out of diffusing particles. The quadratic coupling that we have used captures both multibody and fluctuation-induced interactions. While the former is of paramount relevance, the latter is entirely dominated by thermal fluctuations and can be neglected. We see several directions along which we could expand our findings. From a theoretical standpoint, we wish to investigate the effect of varying the details of the correlator (membranes will feature higher derivatives, for instance). Similarly, the particle-field coupling may also involve higher derivatives depending on physical context. We have further assumed protein diffusion to be spin independent, a simplifying assumption that possibly conceals some activity feedback. Exploring the consequences of hydrodynamic effects is also of great relevance. Finally, it would be interesting to investigate such emerging phenomena in experimental systems of active particles, even in athermal macroscopic systems where activity alone might suffice.

We thank Luca Peliti and Julien Tailleur for useful discussions.

[1] *Animal Groups in Three Dimensions: How Species Aggregate*, edited by J. K. Parrish and W. M. Hamner (Cambridge University Press, Cambridge, England, 1997).

[2] T. Vicsek, A. Czirók, E. Ben-Jacob, I. Cohen, and O. Shochet, Phys. Rev. Lett. **75**, 1226 (1995).

[3] M. Ballerini, N. Cabibbo, R. Candelier, A. Cavagna, E. Cisbani, I. Giardina, V. Lecomte, A. Orlandi, G. Parisi, A. Procaccini *et al.*, Proc. Natl. Acad. Sci. U.S.A. **105**, 1232 (2008).

[4] H. Chaté, F. Ginelli, G. Grégoire, and F. Raynaud, Phys. Rev. E **77**, 046113 (2008).

[5] J. Deseigne, O. Dauchot, and H. Chaté, Phys. Rev. Lett. **105**, 098001 (2010).

[6] I. Theurkauff, C. Cottin-Bizonne, J. Palacci, C. Ybert, and L. Bocquet, Phys. Rev. Lett. **108**, 268303 (2012).

[7] M. E. Cates and J. Tailleur, Annu. Rev. Condens. Matter Phys. **6**, 219 (2015).

[8] J. Alvarado, M. Sheinman, A. Sharma, F. C. MacKintosh, and G. H. Koenderink, Nat. Phys. **9**, 591 (2013).

[9] J. Prost and R. Bruinsma, Europhys. Lett. **33**, 321 (1996).

[10] S. Ramaswamy, J. Toner, and J. Prost, Phys. Rev. Lett. **84**, 3494 (2000).

[11] H.-Y. Chen, Phys. Rev. Lett. **92**, 168101 (2004).

[12] H. B. G. Casimir, Proc. K. Ned. Akad. Wet. **51**, 793 (1948).

[13] M. Kardar and R. Golestanian, Rev. Mod. Phys. **71**, 1233 (1999).

[14] M. E. Fisher and P. G. de Gennes, C. R. Acad. Sci., Ser. B **287**, 207 (1978).

[15] C. Hertlein, L. Helden, A. Gambassi, S. Dietrich, and C. Bechinger, Nature (London) **451**, 172 (2008).

[16] A. Ajdari, L. Peliti, and J. Prost, Phys. Rev. Lett. **66**, 1481 (1991).

[17] P. Poulin, H. Stark, T. C. Lubensky, and D. A. Weitz, Science **275**, 1770 (1997).

[18] M. M. Nicolson, Proc. Cambridge Philos. Soc. **45**, 288 (1949).

[19] D. L. Hu and J. W. M. Bush, Nature (London) **437**, 733 (2005).

[20] M. Goulian, R. Bruinsma, and P. Pincus, Europhys. Lett. **22**, 145 (1993).

[21] N. Dan, P. Pincus, and S. A. Safran, Langmuir **9**, 2768 (1993).

[22] P. Dommersnes and J.-B. Fournier, Eur. Phys. J. B **12**, 9 (1999).

[23] A.-F. Bitbol, D. Constantin, and J.-B. Fournier, PLoS One **7**, e48306 (2012).

[24] C. van der Wel, A. Vahid, A. Šarić, T. Idema, D. Heinrich, and D. J. Kraft, Sci. Rep. **6**, 32825 (2016), .

[25] B.-S. Lu, D. S. Dean, and R. Podgornik, Europhys. Lett. **112**, 20001 (2015).

[26] C.-H. Chen and H.-Y. Chen, Phys. Rev. E **74**, 051917 (2006).

[27] H.-Y. Chen and A. S. Mikhailov, Phys. Rev. E **81**, 031901 (2010).

[28] Y. Oono and Y. Shiwa, Mod. Phys. Lett. B **01**, 49 (1987).

[29] Y. Oono and M. Bahiana, Phys. Rev. Lett. **61**, 1109 (1988).

[30] S. Puri and H. L. Frisch, Int. J. Mod. Phys. B **12**, 1623 (1998).

[31] S. C. Glotzer, D. Stauffer, and N. Jan, Phys. Rev. Lett. **72**, 4109 (1994).

[32] S. C. Glotzer, E. A. Di Marzio, and M. Muthukumar, Phys. Rev. Lett. **74**, 2034 (1995).

[33] R. Krishnan and S. Puri, Phys. Rev. E **92**, 052316 (2015).

[34] P. F. Fribourg, M. Chami, C. O. S. Sorzano, F. Gubellini, R. Marabini, S. Marco, J.-M. Jault, and D. Lévy, J. Mol. Biol. **426**, 2059 (2014).

[35] A. Moeller, S. C. Lee, H. Tao, J. A. Speir, G. Chang, I. L. Urbatsch, C. S. Potter, B. Carragher, and Q. Zhang, Structure **23**, 450 (2015).

[36] A. Sumino, D. Yamamoto, M. Iwamoto, T. Dewa, and S. Oiki, J. Phys. Chem. Lett. **5**, 578 (2014).

[37] L. Criante, F. Bracalente, L. Lucchetti, F. Simoni, and E. Brasselet, Soft Matter **9**, 5459 (2013).

[38] M. Ravnik, S. Čopar, and S. Žumer, J. Phys. Condens. Matter **27**, 354111 (2015).

[39] S. Komura and D. Andelman, Adv. Colloid Interface Sci. **208**, 34 (2014), special issue in honor of Wolfgang Helfrich.

[40] Z. Bu and D. J. E. Callaway, Adv. Protein Chem. Struct. Biol. **83**, 163 (2011).

[41] See Supplemental Material at http://link.aps.org/supplemental/10.1103/PhysRevLett.121.028001 for simulation details and additional informations on particle interactions.

[42] W. Krauth, *Statistical Mechanics: Algorithms and Computations* (Oxford University Press, New York, 2006), Vol. 13.

[43] D. S. Dean, J. Phys. A **29**, L613 (1996).

[44] K. Kawasaki, Physica (Amsterdam) **208A**, 35 (1994).